# Local Map Generation using Position and Communication History of Mobile Nodes

Shinichi Minamimoto Sae Fujii Hirozumi Yamaguchi Teruo Higashino
*Graduate School of Information Science and Technology, Osaka University*
*1-5 Yamadaoka, Suita, Osaka, 565-0871, Japan*
*Japan Science and Technology Agency, CREST*
{*s-minmmt, s-fujii, h-yamagu, higashino*} @ *ist.osaka-u.ac.jp*

***Abstract*—In this paper, we propose an algorithm to estimate 2D shapes and positions of obstacles such as buildings using GPS and wireless communication history of mobile nodes. Our algorithm enables quick recognition of geography, which is required in broader types of activities such as rescue activities in emergency situations. Nevertheless, detailed building maps might not be immediately available in private regions such as large factories, warehouses and universities, or prepared maps might not be effective due to collapse of buildings or roads in disaster situations. Some methodologies adopt range measurement sensors like infra-red and laser sensors or cameras. However, they require dedicated hardware and actions for the measurement. Meanwhile, the proposed method can create a rough 2D view of buildings and roads using only wireless communication history between mobile nodes and position history from GPS receivers. The results from the experiment conducted in 150m×190m region on our university campus assuming rescue and treatment actions by 15 members have shown that our method could generate a local map with 85% accuracy within 350 seconds. We have also validated the performance of our algorithm by simulations with various settings.**

***Keywords*-wireless ad-hoc connection; GPS; map generation; rescue activity;**

## I. Introduction

Situation awareness is the basis of ubiquitous society. We try to sense or capture physical phenomena like change of temperature and raining, or try to recognize and analyze the forms, locations and behavior of the real world's objects (such as vehicles and pedestrians) and landscape.

We have learned that such situation awareness is also very significant for rescue operations in case that many people are suddenly injured by a large accident or a disaster in small and condensed space. For example, in Japan, we have experienced a very tragic train accident in 2005 where over 100 people died and about 460 people were injured. It is reported that in such a situation, rescue teams need to recognize the positions and conditions of injured people for efficient rescue operations [1]. Our research group has started to design and develop an electronic "triage" system. It continuously senses the vital signs of the injured people and estimates their locations by IEEE802.15.4 ad hoc networks. We are leading this national project involving 5 organizations with several medical doctors and professors in emergency care department [2].

These doctors say that fast recognition of obstacles such as buildings in the region will be very helpful for rescue operations and treatment actions. Therefore, a *local map* of the site, which tells us building and street structure information in a city section, presence of warehouses in a factory, or complicatedly-connected small buildings on university campus, is desired. However, such a local, thus detailed map is not obtained from a public map especially if the region is private property, or even pathways (or streets) may be changed after a disaster. Using digital images of landscape or range information from radar sensors is a possibility to build a map, but dedicated effort (*i.e.* taking pictures or measuring ranges at specific points toward specific directions) to obtain such information is required. It encumbers efficient rescue operations since doctors and rescue workers always need manpower for treatment actions. Thus *automated* acquisition of a local map *without dedicated hardware* is mandatory in such emergency situation.

In this paper, we propose a local map generation algorithm for recognition of an accident site in emergency situation. We assume that each member in rescue teams, called a *mobile node*, is equipped with a GPS receiver and a mid-range communication device like IEEE802.11 or IEEE802.15.4 that can communicate with others several tens of meters away. Since such equipment is very general, the algorithm does not require dedicated devices. The algorithm estimates movable areas and obstacles using position information from GPS receivers and communication logs between mobile nodes. We clarify the challenges in this automated generation of local maps using such simple equipment; we need to take into account that GPS errors and uncertainty of radio propagation with presence of obstacles may have negative effect on map accuracy. To cope with this problem, we conducted several preliminary field experiments. Based on the results, we take an approach using probabilities and counters in order to determine whether each sub-region is occupied by an obstacle or is in movable space. After generating rough form of obstacles, image processing techniques are applied to increase the readability of the map.

A field experiment and several simulation experiments were conducted to validate the effectiveness of the algorithm. Especially, in the field experiment, we have generated a local map of 150m×190m region on our university campus.

978-1-4244-5328-3/09/$25.00 ©2009 IEEE

The results from those experiments have shown that the maps with about 85% accuracy were generated within 350 seconds.

## II. Related Work

Recognizing shapes, materials and positions of objects using cameras and sensors has been considered in many application domains for different purposes. In the Intelligent Transport Systems (ITS), many methodologies have been designed for vehicles to recognize obstacles and pedestrians to assist safe driving. For example, Ref. [3] proposes a method that identifies pedestrians and obstacles on roads using stereo cameras and range measurement sensors like infra-red sensors and laser sensors.

Also, in the robotics area, Simultaneous Localization and Mapping (SLAM) techniques [4], [5] are considered important to control the movement of autonomous robots in unknown environments like disaster scenes. These SLAM techniques build maps of surroundings and simultaneously estimate the positions of mobile robots. The methods in Refs. [4], [5] assume that each robot has cameras, range measurement sensors and gyroscope, and the robot creates local maps using the information from these devices. Then the methods create an entire map of the environment by fusing the local maps based on the positions of mobile robots estimated by dead reckoning. In this way, the SLAM methods require accurate distance to obstacles and considerable computation power to process enormous amount of data from the devices.

Meanwhile, some methods of localizing nodes in sensor networks try to estimate such topology that involves "holes" where no node exists and no communication occurs over them [6], [7]. However, it is designed for sensor networks with a large number of stationary nodes. Therefore it is very difficult to apply them to our problem.

Our contribution is two-fold. First, we only use ad hoc wireless communication devices and GPS receivers of mobile nodes. Since they are very general nowadays and they do not require dedicated actions for measurement, it can be used in rescue operations [2] or many other cases. Secondly, estimating obstacle maps using those devices is a very new and challenging problem. For this problem, we have developed an efficient and practical algorithm using both position and communication history of mobile nodes, incorporating image processing techniques.

## III. Problem Statement and Algorithm Design

### A. Problem Statement

In Fig. 1, we exemplify the environment where our algorithm works. A targeted region consists of movable space such as pathways, and obstacles such as buildings. We assume that a *mobile node* (or simply a *node*) is a person who has a wireless terminal and can move only in movable space. Each node has a GPS receiver and

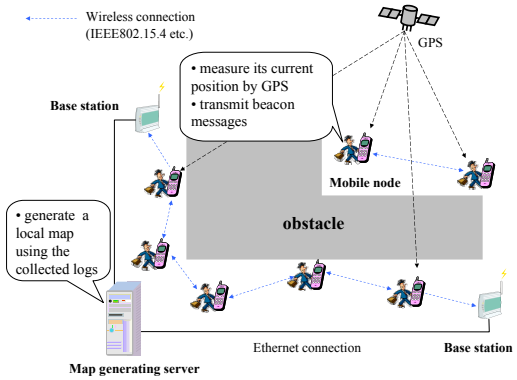


Figure 1. Environment for proposed algorithm.

periodically measures its current position. This position information contains some error range, which is unknown in the algorithm. It also has a mid-range communication device such as IEEE802.11 and IEEE802.15.4. After every position measurement, it transmits a *beacon message* that contains the measured position. We assume that each node roughly knows global time that is easily obtained from its GPS receiver.

Every time node $i$ measures its position, it records $(i, p_i, t)$ where $p_i$ and $t$ are the measured position and time, respectively. This is called a *GPS log*. In addition, when node $j$ receives a beacon message from node $i$ that contains $p_i$, node $j$ records $(i, j, p_i, p_j, t)$ where $t$ denotes the reception time of this message (global time) and $p_j$ is the latest measured position of node $j$. This is called a *communication log*. Both the GPS logs and communication logs collected by mobile nodes are aggregated on a single server. We assume that delivery of those logs is done in some ways; for example, mobile nodes can give them to their base stations when they can communicate with the base stations or by multi-hop transmission over the mobile nodes. On the server, our algorithm estimates the shapes and positions of obstacles.

The problem treated in this paper is to estimate the movable space and obstacles in a targeted area as accurately as possible using all the GPS logs and communication logs.

### B. Map Generation – Challenges and Approaches

We propose a centralized algorithm. The outline of our algorithm is shown by the produced maps in Fig. 2. The algorithm consists of two independent map estimation procedures; (i) estimation of movable space by GPS logs (called *GPS-based estimation procedure*, map (a) of Fig. 2) and (ii) estimation of obstacles by communication logs (called *communication-based estimation procedure*, map (c) of Fig. 2). After the GPS-based estimation procedure, an image processing technique called *closing* is applied (map (b)). Finally, two maps (b) and (c) are merged into a single map (d), and then refined by an original image processing technique called *rectangular approximation* (map (e)).

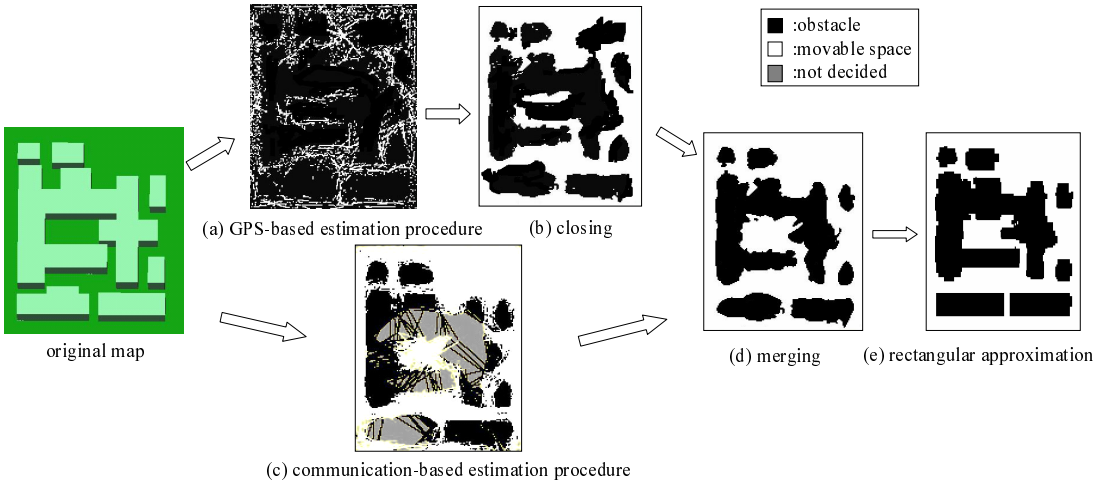


Figure 2. Algorithm outline.

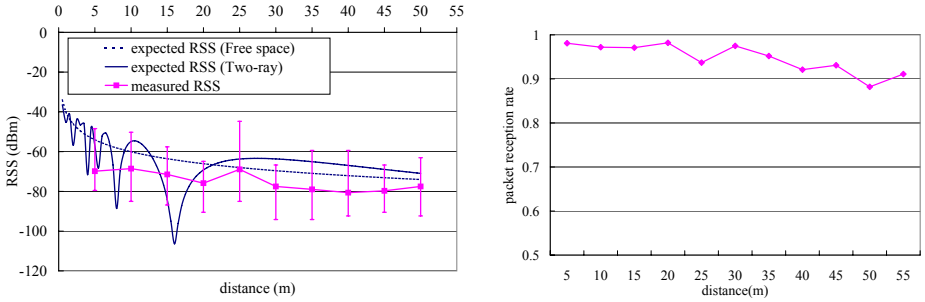


(a) Expected and measured RSS (b) Measured packet reception rate

Figure 3. RSS and packet reception ratio (versus distance).

In the following, we state the design consideration of the two procedures, addressing challenges we face in the problem.

*1) GPS-based Estimation Procedure:* Mobile nodes move in movable space. Therefore, for each GPS log $(i, p_i, t)$, position $p_i$ is in the movable space. In addition, for two time-subsequent logs $(i, p_i, t)$ and $(i, p_i', t+\Delta t)$, the estimated trajectory is also in the movable space. Here, since the positions may have errors, simplistic decision may fail to precisely estimate the movable space. Our approach is a counter-based one where for each small grid cell in the region we count how many times the cell is marked as "movable space". Since GPS errors can be considered quasi-random ones in terms of time, location and nodes, the cells in real movable space will possibly have larger counts. Therefore, this straightforward idea alleviates GPS measurement errors.

*2) Communication-based Estimation Procedure:* One plausible approach for this goal is to consider the received signal strength (RSS). We may derive the expected RSS (denoted as $\hat{rx}$) from a known radio propagation model assuming there is no obstacle between $p_i$ and $p_j$. Then we compare the measured RSS $rx$ with the expected RSS $\hat{rx}$, and see how much $rx$ deviates from $\hat{rx}$. Based on this deviation, we may estimate the existence of obstacles between $p_i$ and $p_j$. However, several factors such as multi-path signals or radio from other sources may interfere with radio propagation and may fluctuate RSS values. For example, for wireless LAN interferes with 2.4GHz radio frequency, human bodies and humidity may also reduce the signal power. In order to observe such phenomena, we have conducted a simple field experiment. We have used ZigBee modules JN5139[8] (Jennic Ltd.). The experiment was done in open space without any obstacle, and two ZigBee modules were set 1m above the ground. One module transmitted 26 bytes packets for every 1 second with transmission power 0 (dBm), and totally 10 packets were transmitted for each distance. Fig. 3(a) shows the expected and measured RSS values versus two nodes' distance. To derive the expected RSS, we have assumed 2.4GHz frequency, and have used the two-ray ground model with $\lambda = 0.125$m and $\gamma = -1$ and the free-space model [9]. From this graph, we can see that the measured RSS values fluctuated even in the same distance case, and do not fit for the models even in this stationary environment. Therefore we can easily conclude

Table I
RSS CALCULATED BY KNIFE-EDGE DIFFRACTION MODEL

| sender \ receiver | | 3 | 4 | 5 | 6 | 7 | 8 | 9 | 10 |
|---|---|---|---|---|---|---|---|---|---|
| 1 | packet reception ratio (%) | 0 | 0 | 0 | 93.3 | 0 | 0 | 0 | 90.7 |
| | expected RSS by diffraction model (dBm) | -108.7 | -104.9 | -99.2 | -90.6 | -112.7 | -109.0 | -103.1 | -93.1 |
| 2 | packet reception ratio (%) | 0 | 13.7 | 59.8 | 94.4 | 0 | 0 | 0 | 91.7 |
| | expected RSS by diffraction model (dBm) | -103.7 | -100.7 | -94.7 | -87.0 | -108.3 | -104.6 | -99.0 | -90.6 |

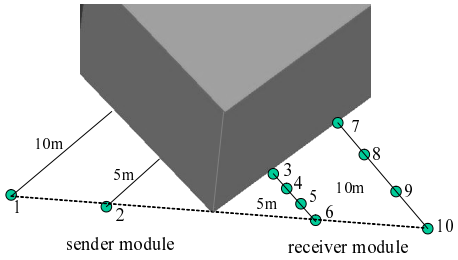


Figure 4. Diffraction propagation.

that they are not applicable in mobile environment we are assuming.

Since RSS is too sensitive, we consider using the packet reception ratio. For two nodes that have shorter distance than the expected maximum communicable range (denoted by $R$), we can estimate the presence of obstacles between two nodes based on the following intuitive rules; (1) if node $j$ could receive a beacon message from node $i$, there is no obstacle between $p_i$ and $p_j$, and (2) if node $j$ could not receive a beacon message from node $i$, there is an obstacle between $p_i$ and $p_j$. However, interference also affects the packet reception ratio as in the case of RSS. For example, a packet is not delivered even if there is no obstacle between $p_i$ and $p_j$ and the distance between them was less than $R$. Another concern is radio diffraction. A packet is delivered even if there is an obstacle between $p_i$ and $p_j$.

In order to see to what extent such phenomena happen, we have also measured the packet reception ratio in the previous experiment of Fig. 3(a). The result is shown in Fig. 3(b). In ideal environment, the packet reception ratio in this graph should be 100%, but actually around 10% is lost due to some reasons. Also, to see the influence of diffraction, we have used Jennic JN5139 (2.4GHz) as in the previous experiment. As shown in Fig. 4, we put two JN5139 modules. The sender was either located at point 1 or 2, and it transmitted 10,000 packets of 26 bytes with -18dBm. The receiver was located at one of points 3-10 and counted the received packets. We note that the RSS threshold of JN5139 was $-96$dBm. The expected RSS was derived using the knife-edge diffraction model [10]. Table I shows the expected RSS values and packet reception ratio. From the results, in any case that the line of sight is blocked by the obstacle, the packet loss ratio was large and diffraction merely occurred. The model indicates that in 2.4GHz RF, the expected RSS was around -95dBm, which is almost the RSS threshold. Since in most cases the measured RSS was smaller than the expected one, packet delivery by diffraction is not likely to occur. Consequently, we can take a simple approach using the packet reception ratio instead of RSS, but we still need to take into account that GPS errors and unexpected loss of packets may obscure the decision. For this, we introduce probability to represent the degree of likelihood that the packet delivery is done as expected. Also, to increase the confidence, we introduce counters as we did in the movable space estimation procedure.

In the following section, we give the details of the algorithm.

## IV. ALGORITHM DESCRIPTION

The algorithm divides a targeted area into $m \times n$ square cells, and estimates for each cell whether it is occupied by an obstacle or not. Hereafter, a cell occupied by an obstacle is called an *obstacle cell* and one in movable space is called a *non-obstacle cell*. A cell at row $a$ and column $b$ is denoted by $g_{a,b}$ ($1 \leq a \leq m$ and $1 \leq b \leq n$).

### A. GPS-based Estimation Procedure

In GPS-based estimation procedure, for each GPS log $(i, p_i, t)$, we find the cell containing $p_i$. In addition, for two subsequent GPS logs $(i, p_i, t)$ and $(i, p_i', t+\Delta t)$, we find the cells on the line segment $p_i$-$p_i'$.

Here, we denote each of such cells by $c$. $c$ might be likely to be a non-obstacle cell, but it should not be the final decision due to ambiguity from GPS errors. Hence, we determine that $c$ is a non-obstacle cell only if mobile nodes transit over cell $c$ more than $h$ times, where $h$ is the average number of mobile nodes' transits over the cell. Here, we explain how to determine the value of $h$. We let $N$, $T$ and $V$ denote the number of mobile nodes, the time length during which logs are collected, and the average speed (m/s) of mobile nodes, respectively. Also the area is $x \times y$ (m$^2$) and the side length of a cell is denoted by $g$ (m). Since the expected time for a mobile node to transit from a cell to its neighboring cell is $g/V$ (s), the expected number of cells all the nodes transit during time $T$ is $TVN/g$. Also, since the number of cells in the targeted area is $xy/g^2$, the average number of mobile nodes' transits per cell is derived by $h = gTVN/xy$.

Finally, to prevent non-obstacle cells, over which few nodes transit, from being determined as obstacle cells, we

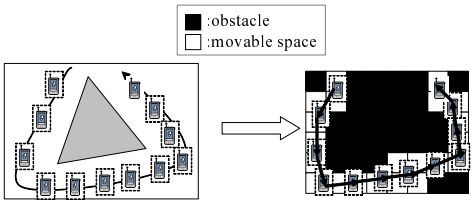


Figure 5. GPS-based estimation procedure.


Figure 6. Closing technique.

apply the *closing* process, which is known as an image processing technique [11]. Closing is used to reveal thin-line characters and lines in figures, and consists of two steps, dilation and erosion of white pixels. In our algorithm, we regard obstacle cells as black pixels, and non-obstacle cells as white pixels. In the dilation step, for each black pixel, it is changed to a white pixel if it has more than five white pixels as its adjacent cells. In the erosion step, for each white pixel, it is changed to a black pixel if it has less than four black pixels as its adjacent cells. We apply the dilation $k$ times, and after that apply the erosion $k$ times (empirically $k = 3$ produces good results). Fig. 5 and Fig. 6 show examples of GPS-based estimation and closing, respectively.

### B. Communication-based Estimation Procedure

In the communication-based estimation procedure, for each cell $g_{a,b}$, we prepare two integer counters $T_{a,b}$ and $F_{a,b}$ initialized by zero. For each pair $(i, p_i, t)$ and $(j, p_j, t)$ of two GPS-logs where the distance between two nodes is less than the maximum communicable range $R$, we check if the corresponding communication log $(i, j, p_i, p_j, t)$ exists or not. If exists, for each cell $g_{a,b}$ on the line segment $p_i$-$p_j$, we increase $F_{a,b}$ by one. Otherwise we increase $T_{a,b}$ by one. Here, $T_{a,b}$ is the count judging that $g_{a,b}$ is an obstacle cell, and $F_{a,b}$ is the one judging that it is a non-obstacle cell. Fig. 7 shows an example of the communication-based estimation procedure.

Based on $T_{a,b}$ and $F_{a,b}$, we determine if $g_{a,b}$ is an obstacle cell or not. Here, there is a possibility that $T_{a,b}$ is increased but $g_{a,b}$ is actually a non-obstacle cell. In opposite, there is also a possibility that $F_{a,b}$ is increased but $g_{a,b}$ is actually an obstacle cell. Because GPS positions include errors and radio propagation is uncertain, such incorrect decision may happen. Therefore, we cannot rely only on those counters.

To cope with such ambiguity, our algorithm calculates the probability that $g_{a,b}$ is an obstacle cell based on Bayesian estimation. Bayesian estimation is a method to estimate the event of a hypothesis from a given observed event. Here we

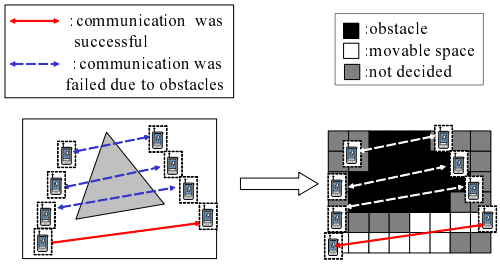


Figure 7. Communication-based estimation procedure.

define $A$ as the event that two nodes communicate with each other over a cell, and $B$ as the event that the cell is actually an obstacle cell. Also, $P(A)$ and $P(B)$ are the probabilities of events $A$ and $B$, respectively. Therefore, $P(B|A)$ is the posterior probability that the cell is an obstacle cell after we know that two nodes communicate over it. $P(B|A)$ is given by formula (1) according to the Bayesian theorem.

$$\begin{aligned} P(B|A) &= \frac{P(A|B)P(B)}{P(A)} \\ &= \frac{P(A|B)P(B)}{P(A|\bar{B})P(\bar{B}) + P(A|B)P(B)} \end{aligned} \quad (1)$$

We may assign 0.5 to the prior probability $P(B)$ because we cannot initially know whether or not each cell is an obstacle cell. If we do so, formula (1) is reducted to formula (2) knowing $P(A|\bar{B}) + P(A|B) = 1$.

$$P(B|A) = 2P(A|B)P(B) \quad (2)$$

From formula (2), the probability that a cell is an obstacle cell is the prior probability multiplied by $2P(A|B)$ when two nodes are regarded communicable over the cell.

In a similar way, we represent $P(B|\bar{A})$, the posterior probability that a cell is an obstacle when nodes are regarded non-communicable over the cell by formula (3). Also the probability that a cell is an obstacle cell is the prior probability multiplied by $2P(\bar{A}|B)$ when two nodes are regarded non-communicable over the cell.

$$\begin{aligned} P(B|\bar{A}) &= \frac{P(\bar{A}|B)P(B)}{P(\bar{A})} \\ &= \frac{P(\bar{A}|B)P(B)}{P(\bar{A}|\bar{B})P(\bar{B}) + P(\bar{A}|B)P(B)} \\ &= 2P(\bar{A}|B)P(B) \end{aligned} \quad (3)$$

By the fact that nodes communicate over a cell, the probability that the cell is an obstacle cell is increased by $2P(A|B)$. Similarly, by the fact that nodes do not communicate over a cell, the probability that the cell is a non-obstacle cell is increased by $2P(\bar{A}|B)$. Based on this idea, we define score $p_{a,b}$ given by formula (4) to determine whether cell $g_{a,b}$ is an obstacle cell or not, using $T_{a,b}$ and

$F_{a,b}$. If $p_{a,b}$ is greater than a certain threshold, we determine that $g_{a,b}$ is an obstacle cell (empirically, 0.8 is appropriate to the threshold).

$$p_{a,b} = \frac{1}{2} \times (2P(A|B))^{T_{a,b}} \times (2P(\bar{A}|B))^{F_{a,b}} \quad (4)$$

In the experiments in the following sections, we have assigned 0.1 to $P(A|B)$ from the preliminary experiment in Section III-B because we can see that the probability that two nodes communicate by diffraction is low when there is an obstacle between them. Also, we assign 0.9 to $P(\bar{A}|B)$ based on the results of received-rate in Section III-B. When $4.5 \times T_{a,b} \leq F_{a,b}$ holds, it is determined that $g_{a,b}$ is an obstacle cell. We note that if both $T_{a,b}$ and $F_{a,b}$ are zero, we do not make decision for $g_{a,b}$.

### C. Merging Maps and Refinement

Finally, we obtain a single map by merging two maps from the above two procedures. The decision for $g_{a,b}$ is done as follows.

- If $g_{a,b}$ is determined as an obstacle cell in both procedures, $g_{a,b}$ is determined as an obstacle cell.
- If $g_{a,b}$ is determined as a non-obstacle cell in both procedures, $g_{a,b}$ is determined as a non-obstacle cell.
- If $g_{a,b}$ is determined as a non-obstacle cell by either one of the two procedures, $g_{a,b}$ is determined as a non-obstacle cell.
  One reason for this rule is that in the communication-based estimation procedure, "non-obstacle" decision is more credible than "obstacle" decision because all the cells between two nodes that cannot communicate with each other are determined as obstacle cells even though most of them are actually non-obstacle ones. Another reason is that in the GPS-based estimation procedure, cells over which nodes do not transit are determined as non-obstacle cells even though they are actually obstacle cells.
- If decision is not made to $g_{a,b}$ in the communication-based estimation procedure, we rely on the decision by the GPS-based estimation procedure.

The obtained map is likely to be distorted as shown in Fig. 2(d). If the forms of buildings are assumed to be close to polygons, we may apply the final refinement procedure called *rectangular approximation*. The procedure recognizes a (small) set of cells that constitute a single obstacle, and approximates its boundaries by lines.

We note that we can exploit existing maps or satellite images, even though they cannot present the latest geography nor detailed structure of buildings, to speedup the algorithm execution and to enhance the accuracy of the results. For example, considering the fact that building are obstacles even if they have collapsed, we can pre-generate an obstacle map based on a given map that tells us the presence of buildings, and can apply our algorithm to estimate their change of shape in details.

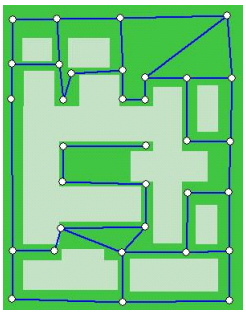

Figure 8. Obstacles in simulation.

Figure 9. Picture of the region.

## V. Performance Evaluation

We have evaluated the performance of our proposed algorithm by simulations using the QualNet simulator [12] and Wireless InSite module [13]. In order to test the performance in such situation that radio is interrupted by obstacles like buildings and the mobility of nodes is restricted, we use a map shown in Fig. 8 that models 150m $\times$ 190m region on our university campus (the picture of the region is shown in Fig. 9). We assume that each mobile node moves along a pathway and randomly chooses a new direction except backward at each intersection, and the speed follows the normal distribution with mean 1.5 m/s and variance 0.01. In order to simulate the radio propagation accurately, we have used the radio propagation model provided by Wireless InSite assuming 2.4GHz RF. Also, we set its transmission power to such a value that makes the maximum radio range be $R_{max}$ according to the two-ray ground model [9]. We note that in this simulator with the radio propagation model, interference affected by multi-path signals are simulated. Moreover, we assume that GPS errors follow the normal distribution with mean $\mu$ and variance 1. The size of a cell was set to 1m$\times$1m, and the maximum communicable range $R$ was equal to $R_{max}$. We set $P(A|B)$, the probability that a cell is an obstacle cell when two nodes communicated over the cell, to 0.1. Also $P(\bar{A}|B)$, the probability that a cell is a non-obstacle cell when two nodes communicated over the cell, was set to 0.9 based on the preliminary experiments in Section III-B. The other parameter settings are shown in Table II (the default values are emphasized by bold font).

In the above settings, we have generated a local map using the GPS logs and communication logs during 600 seconds, and evaluated the ratio of cells estimated correctly to the entire cells. This ratio is denoted by $Hit$ and defined as follows;

$$Hit = \frac{1}{mn} \sum_{a=1}^{m} \sum_{b=1}^{n} hit(g_{a,b})$$

where $m$ is the number of cells in row and $n$ is that in column. $hit(g_{a,b})$ returns 1 if $g_{a,b}$ is estimated correctly, and returns 0 otherwise.

Table II
SIMULATION SETTING

| | |
|---|---|
| maximum radio range ($R_{max}$) | 25 ,**50**, 75 (m) |
| number of mobile nodes | **15**, 30 ,45 |
| beacon message transmission frequency ($T_c$) | **1.0**, 5.0, 10.0 (s) |
| GPS positioning frequency ($T_p$) | **1.0**, 5.0, 10.0 (s) |
| average position error ($\mu$) | 0, **5.0**, 10.0 (m) |

(a) $R_{max} = 25$ (b) $R_{max} = 50$ (c) $R_{max} = 75$

Figure 10. Generated maps under different $R_{max}$ values.

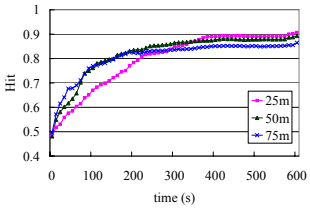


Figure 11. Impact of $R_{max}$ on $Hit$.

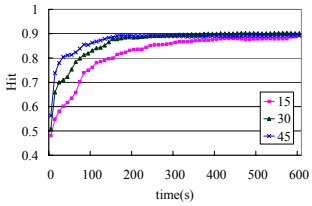


Figure 12. Impact of the number of nodes on $Hit$.

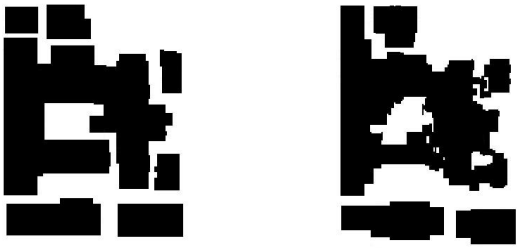

(a) $\mu$ = 0m (b) $\mu$ = 10m

Figure 13. Generated maps under different position errors.

### A. Impact of Parameters on Estimation Accuracy

We have evaluated the impact of several factors on estimation accuracy. We have varied one of parameters in Table II, and set the other parameters to the default values.

*1) Maximum communicable range:* We have observed $Hit$ under different transmission powers such that $R_{max}$ in ideal environment was 25m, 50m or 75m. Fig. 10 shows the generated maps, and Fig. 11 shows $Hit$. We can see that the estimation accuracy is better as the range is shorter. This is because our algorithm regards all the cells over the line segment between two nodes that are closer than $R_{max}$ as obstacle cells if they cannot communicate with each other. The number of incorrect cells with short radio range is smaller than that with long radio range.

*2) Number of mobile nodes:* Then we have varied the number of nodes. Fig. 12 shows the result when the number of nodes was set to 15, 30 or 45. We can see that, with the larger number of nodes, $Hit$ is larger and converges quickly. This is simply because we can get more GPS logs and communication logs.

*3) Beacon message frequency:* We have varied the beacon message frequency denoted by $T_c$. It was set to 1, 5 or 10 seconds. The result is shown in Fig. 14. We can see that the larger frequency results in smaller $Hit$ due to less amount of information about communication. However, $Hit$ is larger than 0.8 even in case that frequency $T_c$ is 10.

*4) Average position error:* GPS errors will greatly affect the accuracy since it affects both the GPS-based and communication-based estimation procedures. We have set the average of position errors to 0, 5 or 10m and measured $Hit$. Fig. 13 shows the generated maps, and Fig. 15 shows the corresponding values of $Hit$. It is natural that the value of $Hit$ under a smaller position error is better. However, even in case of 10m, we can obtain a readable map and this can further be improved by applying the image processing techniques (like Closing) several times more.

*5) GPS positioning frequency:* We have also evaluated $Hit$ varying the GPS positioning frequency $T_p$. It was set to 1, 5 or 10 seconds. From Fig. 16, the GPS positioning frequency has little effect on estimation accuracy since we conducted linear interpolation of trajectory when the frequency was long.

### B. Effect of each estimation procedure

In this section, we have evaluated effects of the GPS-based and communication-based estimation procedures. We have compared the three maps obtained by the GPS-based estimation procedure, by the communication-based estimation procedure, and by both procedures (the final product of our algorithm). We have used the same setting as the previous experiment.

From Fig. 17, we can see that the final map is the most accurate. The estimation accuracy of the GPS-based one is monotonically increasing, but it is not sufficient for practical use. Similarly, that of the communication-based one is increasing, but it does not reach the final result. This indicates the necessity of both procedures, and combination of the results from them yields good results.

### C. Discussion on Communication Logs

In this section, we discuss the amount of communication logs to achieve enough accuracy. We revisit the result in Fig. 11. In all the cases of $R_{max}$, estimation accuracy is convergent when we use communication logs for more than

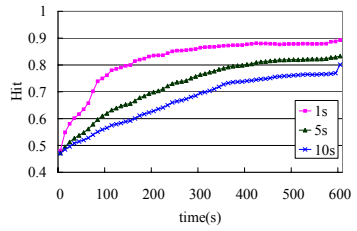


Figure 14. Impact of beacon message frequency $T_c$.

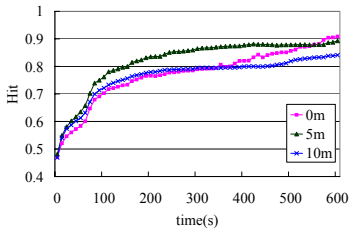


Figure 15. Impact of average position error $\mu$.

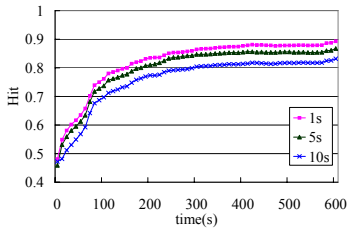


Figure 16. Impact of GPS positioning frequency $T_p$.

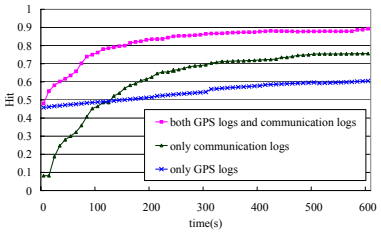


Figure 17. Performance of each procedure.

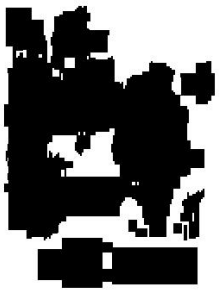

(a) using native GPS logs ($Hit$=0.77).

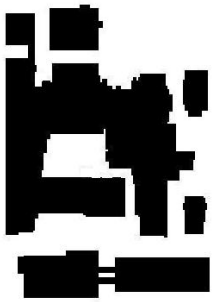

(b) using corrected GPS logs ($Hit = 0.86$).

Figure 18. Generated maps

Table III
ANALYSIS OF COMMUNICATINO LOGS.

| real experiment \ simulation | success | failure |
|---|---|---|
| success | 91.1 (%) | 6.4 (%) |
| failure | 8.8 (%) | 93.6 (%) |

300 sec., which corresponds to 4,000 communication logs. In order to evaluate the time to obtain 4,000 communication logs, we have conducted simulation varying the number of nodes (15, 30 and 45). The other parameters are set to the values in Table II. When we have 15, 30 and 45 nodes, it took 352 sec., 143 sec. and 94 sec., respectively, to obtain more than 4,000 communication logs. From the results, our algorithm can generate a local map with 85% accuracy only assuming 15 members' GPS logs and communication logs for 350 seconds. Therefore we can say that our method is realistic and useful because our algorithm is applicable to disaster cases or others.

## VI. PERFORMANCE EVALUATION IN REAL ENVIRONMENT

In order to evaluate the performance in real environment, we have conducted the experiment in 150m $\times$ 190m region on Osaka University campus shown in Fig. 9. We let each person (mobile node) have Jennic JN5139 [8] (IEEE802.15.4 module) and IO-DATA USBGPS22 [14] (GPS receiver). Each person moved along a pathway and randomly chose a direction (except backward) at each intersection. The moving speed was about 1.5 m/s. It also sent beacon messages and measured the positions by GPS every second ($T_c = T_p = 1$ sec.) with the transmission power $-18$dBm. In our algorithm, the maximum communicable range $R_{max}$ is about 50m. For the other parameters, we have used the same setting as the simulation experiments in Section V. The size of a cell was set to 1m $\times$ 1m, $P(A|B)$ was set to 0.1, and $P(\bar{A}|B)$ was set to 0.9. We have collected GPS logs and communication logs of ten persons for 600 seconds, and evaluated $Hit$, the ratio of the cells estimated correctly to the entire cells.

Fig. 18(a) illustrates the map generated by our algorithm using native GPS positions. Also, $Hit$ is 0.77, which is much lower than the result from the simulation (about 0.9).

To see the problem, we have compared the communication logs in real environment and in simulation. Table III shows the ratio of correspondence of success/failure of communications in simulation and in real environment. "failure" means that communication between two nodes was failed even though they were closer than distance $R_{max}$, and otherwise it is regarded as "success". From Table III, we can see that more than 90 % logs were identical, which seems a good result.

Therefore, we have analyzed the GPS logs. The "native GPS" values in Table IV show the distribution of the measured GPS position errors. From the result, we can say that some GPS logs contain large errors (more than 50m), which may impact on estimation accuracy seriously. This is because some nodes cannot receive GPS signal accurately

Table IV
ANALYSIS OF GPS LOGS

| position error (m) | native GPS | corrected GPS |
|---|---|---|
| 0 - 5 m | 4742 | 4853 |
| 5 - 10 m | 1996 | 2191 |
| 10 - 15 m | 948 | 1106 |
| 15 - 20 m | 605 | 627 |
| 20 - 25 m | 361 | 201 |
| 25 - 30 m | 150 | 7 |
| 30 - 35 m | 82 | 0 |
| 35 - 40 m | 49 | 0 |
| 40 - 45 m | 6 | 0 |
| 45 - 50 m | 1 | 0 |
| 50 - m | 45 | 0 |

due to buildings. Then we try to eliminate such large position errors considering their prior and posterior positions. We correct them so that they are on the lines between their prior and posterior positions. The distribution of position errors is shown as "corrected GPS" of Table IV. We can see that position errors of GPS logs are improved (the average position error is 6.33m). Also, we generate a local map using the modified GPS logs, and evaluate estimation accuracy of the map. The generated map using this corrected GPS logs is shown in Fig. 18(b), which has similar $Hit$ value (0.86) with the simulation experiment. From these results, it is concluded that accurate position information is important, and it can be obtained by simple filtering that eliminates outliers.

In our algorithm, we assume that nodes can measure their current positions using GPS recievers, but GPS may not work in such a place where many buildings interrupt signals from satellites. In order to solve this problem, we may use range-free localization that only uses wireless connectivity information (for example, see Ref. [15]).

## VII. CONCLUSION

We have proposed an algorithm to estimate the shapes and positions of obstacles using mobile nodes' ad hoc communication devices and GPS receivers. Our proposed algorithm estimates movable space and obstacles using GPS logs and communication logs, and refines the result by applying some image processing procedures to obtain a readable map. Through several experiments in simulations and real environment, we have shown that our algorithm could generate readable and accurate maps.

As we stated in Section I, medical doctors and rescue workers say that geography information is very important in rescue and treatment actions in emergency situation. Therefore, in our ongoing project [2], we are trying to incorporate this algorithm into our "electronic triage system" for instant and automated generation of local maps. We will also conduct more experiments in real environments to assess the scalability and availability of our algorithm. This is part of our ongoing work.

## ACKNOWLEDGMENT

This research was partially supported by Research and Development Program of 'Ubiquitous Service Platform' (2009), The Ministry of Internal Affairs and Communications, Japan.

## REFERENCES

[1] Japanese Association for Disaster Medicine, *Japanese Jounal of Disaster Medicine*. Herusu Publishing, 2007, vol. 12, no. 1, (In Japanese).

[2] T. Higashino, "Advanced wireless communication technology for efficient rescue operations," Japan Science and Technology Agency, [Online]. Available: http://www.jst.go.jp/kisoken/crest/en/area02/1-04.html.

[3] T. Gandhi and M. M. Trivedi, "Pedestrian protection systems: Issues, survey, and challenges," *IEEE Transactions on Intelligent Transportation Systems*, vol. 8, no. 3, pp. 413–430, 2007.

[4] H. Choset and K. Nagatani, "Topological simultaneous localization and mapping (SLAM): towardexact localization without explicit localization," *IEEE Transactions on Robotics and Automation*, vol. 17, no. 2, pp. 125–137, 2001.

[5] H. Durrant-Whyte and T. Bailey, "Simultaneous localization and mapping: part I," *IEEE Robotics & Automation Magazine*, vol. 13, no. 2, pp. 99–110, 2006.

[6] Y. Wang, J. Gao, and J. S. B. Mitchell, "Boundary recognition in sensor networks by topological methods," in *Proc. of MobiCom 2006*, 2006, pp. 122–133.

[7] S. Funke, "Topological hole detection in wireless sensor networks and its applications," in *Proc. of the 2005 joint workshop on Foundations of mobile computing*, 2005, pp. 44–53.

[8] Jennic Ltd., "JN5139 IEEE802.15.4/JenNet Evaluation Kit," [Online]. Available: http://www.jennic.com/products/development_kits/jn5139_ieee802154_jennet_evaluation_kit.

[9] J. D. Parsons, *The mobile radio propagation channel*. Wiley, 1992.

[10] W. C. Y. Lee, *Mobile communications engineering*. McGraw-Hill Professional, 1982.

[11] J. C. Russ, *The image processing handbook*. CRC press, 2006.

[12] Scalable Network Technologies, "QualNet," [Online]. Available: http://www.scalable-networks.com/products/qualnet/.

[13] Remcom, "Wireless InSite," [Online]. Available: http://www.remcom.com/wireless-insite.

[14] I-O DATA INC., "USBGPS2 web page," [Online]. Available: http://www.iodata.jp/product/mobile/gps/usbgps2/ (In Japanese).

[15] S. Fujii, T. Nomura, T. Umedu, H. Yamaguchi, and T. Higashino, "Real-time trajectory estimation in mobile ad hoc network," in *Proc. of MSWiM2009*, 2009, pp. 163–172.